Sustainable cooling alternatives for buildings

Jaco Vorster

Robert Dobson

Department of Mechanical & Mechatronic Engineering, University of Stellenbosch, South Africa

Abstract

Four sustainable alternative-energy cooling system options are investigated to quantify the actual energy that may be saved when employed in conjunction with conventional air conditioning systems. The four systems considered are active mass cooling, night flushing, roof-spraying and a roof-pond. A one-room building configuration is assumed of which the hourly cooling load and temperature is modelled for both a base case and different combinations of the four sustainable cooling alternative systems. Active mass cooling, night flushing and the roof-spray system proved to be viable options in which the cooling load of an air conditioner may be reduced to maintain a constant room temperature. The roof-spray system showed the most effective results in limiting heat gains to the one-room building and keeping peak room temperatures low.

Keywords: night flushing, active mass cooling, roof-spray, roof-pond, cooling load

1. Introduction

The World Business Council of Sustainable Development estimates that a third of the world's energy is consumed in the production and operation of buildings (WBCSD, 2009). Air conditioning accounts for more than 50% of the total energy consumed by buildings. The energy consumption of air conditioning systems can thus be significantly reduced by minimising the heat gains to buildings. Several options, in addition to architectural and material changes, are available in which the heat gains to buildings may be reduced. These options will be referred to as sustainable cooling alternatives due to their ability to enhance building energy efficiency and reduce environmental impact.

The sustainable cooling options considered in this paper, namely a roof-pond, a roof-spray, active mass cooling and night flushing were not randomly chosen, but were selected based on the outcome of a carefully structured questionnaire sent to various industry stakeholders (see Appendix A). The outcome of the survey questionnaire showed that night flushing and active mass cooling had the highest degree of commercialization since they are the most likely to be specified by the client or consultant alike. The roof-pond and roof-spray systems were selected due to their ability to reduce building heat gains through the roof and produce cool water during the night time. The cool water may then in turn be employed in a pre-cooling coil of an air conditioning unit or even in an active mass cooling system.

Numerous literature studies have been undertaken to quantify the benefit of a roof-pond, roof-spray, active mass cooling and night flushing applied to a building. Some of this literature will be reviewed in Section 2.

In Section 3 a one-room building is defined and then used to mathematically model and compare the sustainable cooling alternative options. The mathematical model of each of the four sustainable cooling alternatives is given in Section 4. Section 5 gives the temperature and cooling load profile of the one-room building when these models are incorporated in the one-room building model. Having achieved the objective of mathematically modelling the one-room building and the various sustainable cooling alternative options the following could be determined:

- Quantification of the peak cooling load reduction that may be achieved from the one-room building base case for each sustainable energy cooling alternative option.
- Quantification of the peak room temperature reduction that may be achieved from the base case for each sustainable cooling alternative options.

- An estimate of the total energy that may be saved that would otherwise have been consumed by the air conditioning system.
- Comparison of the various sustainable cooling alternatives to the same reference system and for the same input conditions.

By systematically and quantitatively comparing the sustainable cooling alternatives to the same reference system, the most beneficial sustainable cooling system in terms of energy efficiency and CO_2 footprint may be determined with confidence.

2. Literature review

The roof-pond, roof-spray, night flushing and active mass cooling options are considered and each will be reviewed in the following sub-sections.

2.1 Roof-pond and roof-spray

According to Abernethy (1984) the first roof-spray system was introduced in Washington D.C. in 1934 when an irrigation engineer designed and installed a roof-spray system on the roof of a three story apartment building to reduce heat gains. In 1939 the American Society of Heating & Ventilating Engineers conducted extensive tests on roof-spray systems and found that such a system can reduce peak roof heat gain penetration by 87% and average roof heat gain penetration by 92%.

Chandra *et al.* (1985) conducted a periodic heat transfer analysis to predict the dynamic behaviour of a non-air-conditioned building with evaporative cooling systems over the roof. The three types of evaporative cooling systems considered were an open roof-pond, a moving water layer over the roof and a water spray over the roof. From the analysis it was found that maximum cooling was achieved by the water spray system on the roof. This corresponds to the experimental findings of Jain and Rao (1974) who concluded that the roof-spray would reduce the roof temperature more than that of an open roof-pond.

Both Holder (1957) and Thappen (1943) pointed out that the load on an air conditioning plant can be reduced by 25% by the implementation of a roof-spray system. Sodha *et al.* (1980) theoretically analysed the reduction of the heat flux entering a room through a roof with an open water pond. It was claimed that the roof-pond reduces the peak heat flux entering a room by 48% compared to the 41% achieved by a water spray system. This result is in disagreement with the finding by Jain and Rao (1974) and Chandra *et al*. (1985) that the roof-spray is more effective than the roof-pond.

2.2 Night flushing

Night flushing is the process whereby a building is flushed with cold ambient air for several hours each night by means of a mechanical ventilation system. This process lowers the heat stored in the building structure such that the space heat gain may be reduced the following day.

Geros *et al.* (1990) reported that the cooling efficiency of night flushing is mainly dependant on the air flow rate, the thermal capacity of the building structure and the efficient coupling of air flow and thermal mass. Pfafferott *et al.* (2003) also emphasized that air flow rate, heat transfer coefficient and heat storage are the crucial factors in modelling and thereby determining night ventilation efficiency. Geros *et al.* (1999) conducted a series of simulations to determine the energy conservation due to night ventilation for a building in Athens named Meletitiki. The simulations were performed for night ventilation air flow rates that varied from 5 to 30 ACH. The greatest energy conservation was achieved for night ventilation at an air change rate of 30 ACH.

Pfafferott *et al*. (2004) evaluated monitored room data of 12 office rooms of a low energy office building in Germany, named the 'DB Netz AG in Hamm'. A detailed simulation, based on the monitored room data, of the building was performed to ascertain the possibility of improved ventilation strategies

Artmann *et al.* (2008) quantified the performance of the night flushing technique by means of overheating degree hours. The overheating degree hours are defined as the number of hours during which the temperature exceeds 26 °C, weighted by degrees by which 26 °C is exceeded.

Artmann *et al*. (2008) simulated the room temperature of a typical office room for climatic conditions in Europe. The office room volume was 52 m^3 with a high peak internal heat gain of 35 W/m^2 and a *medium level* thermal mass. The overheating degree hours above 26 °C for Zurich, London and Paris were 79 Kh/a, 90 Kh/a and 434 Kh/a respectively when night ventilation was applied between 7 pm and 7 am at 6 air changes per hour (ACH).

Artmann *et al.* (2008) also evaluated the effect of the air change rate on the effectiveness of the night flushing technique. It was found that the average overheating hours above 26 °C were reduced from 466 Kh/a to 138 Kh/a when the air change rate was increased from 2 to 8 ACH in a building with medium internal heat gains. For an office building with high heat gains and thermal mass the overheating hours were reduced from 419 Kh/a to 32 Kh/a for a 2 to 8 ACH increase. This agrees with the analysis by Finn *et al.* (2007) who found that thermal comfort levels where significantly increased for air change rates of 4 to 10 ACH with no significant improvement found beyond 10 ACH.

In Artmann's (2008) evaluation of air change rates it was found that the night ventilation air change rate had to be increased from 8 to 32 ACH to yield a reduction of 100 overheating hours per year of an office with a low thermal mass and high

internal heat gains. A further increase in the air change rate did not produce a significant cooling load reduction.

Geros *et al.* (1999) showed experimentally that for a full scale office building in Athens the average overheating hours could be reduced from 1253 to 615 by the application of night ventilation at a rate of 30 ACH.

Blondeau *et al.* (1997) showed experimentally that for a three level office and classroom building in La Rochelle France, the application of night flushing can halve the cooling capacity required for a 26 °C setpoint. In spite of unfavourable meteorological conditions where the average outdoor temperature range was only 8.4 °C the diurnal indoor air temperatures could be decreased between 1.5 °C and 2 °C when night flushing was applied. Geros *et al.* (1999) showed that the peak indoor temperature of an office building could be reduced by 3 °C.

2.3 Active mass cooling

Corgnati and Kindinis (2007) report that the structural mass plays an essential role in the thermal response of a building. Lehmann *et al.* (2007) report that building elements such as structural floors and slabs serve as energy storage whose dynamic thermal behaviour can be exploited to provide either cooling or heating. The higher the thermal mass the smaller the indoor temperature swing and vice versa. The importance of building thermal mass is further highlighted by Givoni (1998) who noted that the effect of night ventilation is very effective for buildings with high thermal mass but not for those buildings with a low thermal mass. Lehmann *et al.* (2007) noted that the use of the building's thermal mass serves to flatten out peaks in energy demand.

The thermal surfaces of the building structure constantly absorb energy from the heat gained by the room and the thermal energy capacity of the building structure is increased. One way to reduce the thermal energy contained in the building mass is to make use of hollow core slab cooling in combination with night ventilation (Corgnati and Kindinis, 2007). With this concept ventilation air is first circulated through the hollow cores of the slab before routed to the room. As an alternative Lehmann *et al.* (2007) as well as Koschenz and Dorer (1999) utilize water as a medium to which energy from the building mass may be rejected. The water flows through a pipe network embedded in the floor or roof-slab of the building.

3. One-room building base case model

From the literature study it is seen that although much has been done for each individual option very little has been done in comparing the efficacy of the various options with each other. Also, the work that has been done on the various options has been performed in different parts of the world with vastly different weather conditions. This further complicates an accurate comparison of the various options. To overcome this difficulty a simple base case model consisting of a one-room building subject to typical weather conditions and heat gains has been assumed. The different energy saving options can then be implemented either singularly or in combination. The energy saving potential, both quantitatively and uniformly, of the various options may then be accurately compared.

The one-room base case model building consists of four 230 mm single brick walls, a 200 mm roof-slab, a north facing window with venetian blinds and a door on the southern wall. The window has an aluminium frame with 6 mm uncoated single glazing. The layout and building dimensions of the one-room building are presented in Figure 1.

The relative cooling efficacy of each of the options either singularly or in various combinations, will be ascertained by comparing their ability to keep such a one-room cool, subject to the same heat gains, to within the same specified temperature limits.

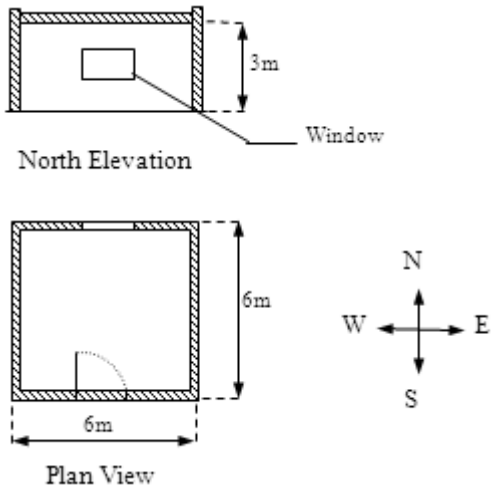

Figure 1: One-room building layout and dimensions

3.1 One-room building mathematical model

The mathematical model for the calculation of the cooling load comprises a set of energy conservation equations applied to those components of the one-room building where room temperature is influenced (e.g. walls, roof-slab etc.). Not all the energy entering the building constitutes an immediate change in room temperature. Take, for example, the heat energy released in the building due to lighting or fenestration. This radiant energy must first strike and be absorbed by a solid surface before some of this energy is released to the space air through convection. The difference between the instantaneous heat gain and the actual space cooling load may be illustrated in Figure 2.

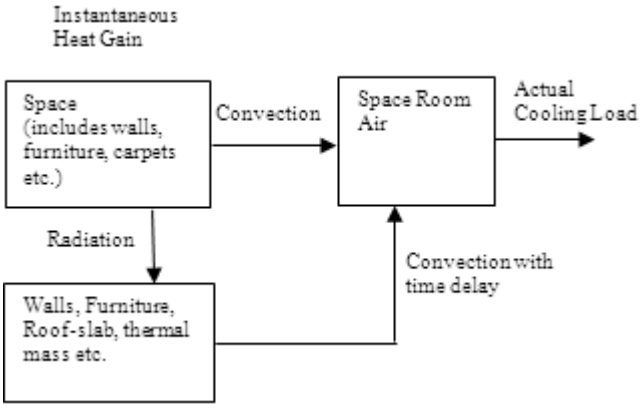

Figure 2: Flowchart illustrating the difference between instantaneous heat gain and actual cooling load
(ASHRAE Fundamentals, 2005)

The instantaneous heat gain refers to the rate at which heat enters into and/or is generated within a space while the actual space cooling load may be seen as the rate at which heat must be removed to maintain a constant space air temperature (ASHRAE Fundamentals, 2005). The time delay between the instantaneous heat gain and the actual space cooling load must be taken into account when performing cooling load calculations (ASHRAE Fundamentals, 2005). To account for the time delay when heat is transferred through the building structure, the walls and the roof-slab of the one-room building are treated as a transient conduction problem. The walls and roof-slab are discretised into a set of control volumes to allow the temperature and heat transfer to be calculated at subsequent time intervals. For the fenestration, lighting and occupancy heat gains the time lag will be taken into consideration by making use of the radiant time series procedure as recommended by ASHRAE.

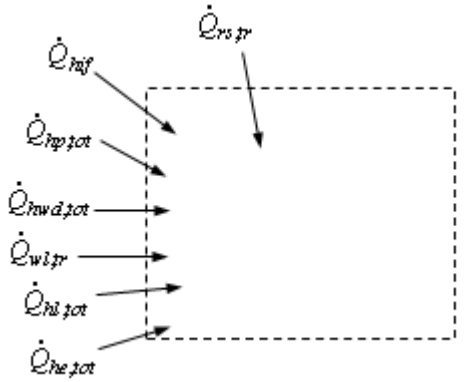

Figure 3: Heat gains to the one-room building space air

Figure 3 depicts the space air control volume of the one-room building with the corresponding heat gain terms. Applying the conservation of energy to the room air control volume gives:

$$m_{rm,a}C_{rm,a}\frac{\partial T_{rm}}{\partial t} = \dot{Q}_{hif} + \dot{Q}_{rs,tr} + \dot{Q}_{wl,tr} + \dot{Q}_{hp,tot} + \dot{Q}_{hwd,tot} + \dot{Q}_{hl,tot} + \dot{Q}_{he,tot} \quad (1)$$

where $m_{rm,a}$ denotes the room air mass, $C_{rm,a}$ the specific heat of the room air at constant pressure, T_{rm} the room temperature, t time, $\dot{Q}_{hif}$ the infiltration energy gain or loss, $\dot{Q}_{rs,tr}$ the roof-slab heat gain, $\dot{Q}_{wl,tr}$ the wall heat gain, $\dot{Q}_{hp,tot}$ the heat gain from the people in the building, $\dot{Q}_{hwd,tot}$ the heat gain through the window, $\dot{Q}_{hl,tot}$ the heat gain from the lighting and $\dot{Q}_{he,tot}$ the heat gain from the room equipment.

The sum of the terms on the right hand side of equation (1) gives the total cooling load, and is dependent on the time. The new room temperature after a time step $T^{t+\Delta t}$ is obtained by expressing the partial differential equation (1) in an explicit finite difference form (Cengel and Boles, 2002)

$$T_{rm}^{t+\Delta t} = T_{rm} + \frac{\Delta t}{m_{rm,a}C_{rm,a}}\begin{pmatrix}\dot{Q}_{hif} + \dot{Q}_{rs,tr} + \dot{Q}_{wl,tr} \\ + \dot{Q}_{hp,tot} + \dot{Q}_{hwd,tot} \\ + \dot{Q}_{hl,tot} + \dot{Q}_{he,tot}\end{pmatrix} \quad (2)$$

where in accordance with the explicit method all the terms on the right hand side are reckoned at the old time (for convenience the superscript "t" has been omitted).

Each heat transfer terms depicted in Figure 3 constitutes an actual cooling load and the procedure for calculating each of these heat transfer terms will be discussed in the next sections.

3.1 Infiltration energy gain or loss

Based on the conservation of energy it can be shown that the infiltration energy gain or loss to the one room building may be calculated by (Cengel and Boles, 2002)

$$\dot{Q}_{hif} = \rho_a \dot{V}\left(C_{p,a} + \omega C_{p,vap}\right)\Delta T \quad (3)$$

where ρ_a is the average air density of the outdoor and indoor air, $\dot{V}$ the infiltration or ventilation volume flow rate, $C_{p,a}$ is the specific heat at constant pressure of dry air, ω the humidity ratio, $C_{p,vap}$ the specific heat of water vapour at constant pressure and ΔT the temperature difference between the indoor and outdoor air.

3.2 Heat gain through a single brick wall

The energy absorbed at the outside surface of the walls is only released to the space air by means of convection some time later due to the low thermal conductivity of the walls. In order to take this thermal delay of the wall structure into account each

thermal delay of the wall structure into account each wall is discretized into a set of one dimensional control volumes as shown in Figure 4.

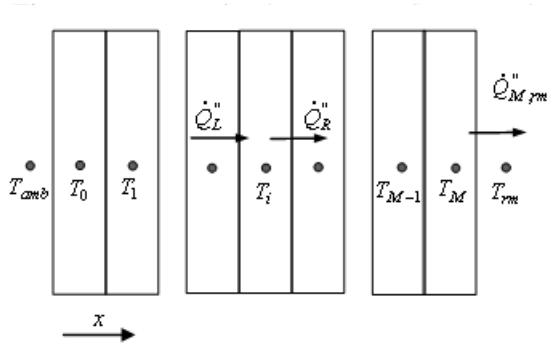

Figure 4: Section of wall with control volumes

The temperature distribution as a function of x and t in the wall is obtained by applying the conservation of energy per unit area to each control volume. For the i^{th} control volume the temperature may be explicitly expressed as

$$T_i^{t+\Delta t} = T_i + \frac{\Delta t}{\Delta x \rho_{sbw} C_{sbw}} \left(\dot{Q}''_L - \dot{Q}''_R \right) \quad (4)$$

where ρ_{sbw} gives the density of the single brick wall, C_{sbw} the specific heat of the wall and Δx the control volume thickness. For an interior node

$$\dot{Q}''_L = -k \frac{\partial T}{\partial x}\bigg| x = x_{i-1/2} = k \frac{T_{i-1} - T_i}{\Delta x} \quad (5)$$

and similarly

$$\dot{Q}''_R = -k \frac{\partial T}{\partial x}\bigg| x = x_{i+1/2} = k \frac{T_i - T_{i+1}}{\Delta x} \quad (6)$$

For the left hand boundary control volume at the 0^{th} node

$$\dot{Q}''_L = \dot{Q}''_{0,solar} - \dot{Q}''_{0,rad} + \dot{Q}''_{0,conv} \quad (7)$$

where $\dot{Q}''_{0,solar} = \alpha_{solar,wl} I_{solar,tot}$, $\dot{Q}''_{0,conv} = h_{conv,o}(T_{amb} - T_0)$, $\dot{Q}''_{0,rad} = \varepsilon_{wl}\sigma(T_0^4 - T_{amb}^4)$ and $\alpha_{solar,wl}$ denotes the wall solar absorptivity, $I_{solar,tot}$ the total solar irradiation comprising reflected, diffuse and beam components, $h_{conv,o}$ the heat transfer convection coefficient between the outer wall surface and the ambient air, T_{amb} the ambient temperature, ε_{wl} the wall emissivity, and σ the Stefan-Boltzman constant.

Forced convection correlations for the calculation of $h_{conv,o}$ apply when assuming an average air velocity of 2 m/s at the outside wall surface of the one-room building. With the one-room building configuration it can be shown that transition from laminar to turbulent flows occurs at approximately the centre of the wall. The appropriate correlation for the calculation of $h_{conv,o}$ is (Incropera & Dewitt, 2002)

$$\overline{Nu}_L = h_{conv,o} L / k_{rm,a} = (0.037 Re_L^{4/5} - 871) Pr^{1/3} \quad (8)$$

where L denotes the width of the wall, $k_{rm,a}$ the air thermal conductivity, Pr the Prandtl number, Re_L the Reynolds number calculated as $Re_L = u_a L / \nu_{amb}$, u_a the ambient air velocity and ν_{amb} the kinematic viscosity of the ambient air.

For the right hand boundary control volume at the M^{th} node

$$\dot{Q}''_R = \dot{Q}''_{M,conv} \quad (9)$$

where $\dot{Q}''_{M,conv} = h_{conv,i}(T_M - T_{rm})$, $h_{conv,i}$ denotes the inner wall surface convection coefficient and T_{rm} the space room temperature. As will be shown in Section 4.1 $h_{conv,i}$ may be calculated by natural convection correlations. In this study the Churchill and Chu natural convection correlation given by equation (30) may be employed. The temperature distribution in the wall may now be calculated for subsequent time intervals.

With the temperature known at the node M, the heat gain $\dot{Q}_{wl,tr}$ transmitted through the walls and transferred to the room space air via convection may be calculated by

$$\dot{Q}_{wl,tr} = h_{conv,i} A_{wl} (T_M - T_{rm}) \quad (10)$$

where A_{wl} denotes the inner wall surface area.

3.3 Heat gain through the roof-slab

Similar to the walls of the one-room building the roof-slab may be discretized into a number of one-dimensional control volumes (see Figure 5) and the temperature for the i^{th} control volume in the roof-slab expressed as

$$T_i^{t+\Delta t} = T_i + \frac{\Delta t}{\Delta x \rho_{rs} C_{rs}} \left(\dot{Q}''_T - \dot{Q}''_B \right) \quad (11)$$

where ρ_{rs} denotes the density of the roof-slab, C_{rs} the specific heat of the roof-slab and Δx the control volume thickness. For the interior roof-slab control volumes $\dot{Q}''_T$ is calculated similarly to $\dot{Q}''_L$ in equation (5). Likewise $\dot{Q}''_B$ is calculated similarly to $\dot{Q}''_R$ in equation (6). For the top control volume in contact with the ambient air and at the 0^{th} node

$$\dot{Q}''_T = \dot{Q}''_{0,solar} - \dot{Q}''_{0,rad} + \dot{Q}''_{0,conv} \quad (12)$$

Where
$\dot{Q}''_{0,solar} = \alpha_{solar,rs} I_{solar,tot}$, $\dot{Q}''_{0,conv} = h_{conv,rs,o}(T_{amb} - T_0)$, $\dot{Q}''_{0,rad} = \varepsilon_{rs}\sigma(T_0^4 - T_{sky}^4)$ and $\alpha_{solar,rs}$ denotes the roof-slab absorptivity, $h_{conv,rs,o}$ denotes the heat transfer coefficient between the outside wall surface and the ambient air, ε_{rs} the roof-slab emissivity and T_{sky} the sky temperature. $h_{conv,rs,o}$ may be calculated using equation (8).

For the roof-slab in contact with the room air

$$\dot{Q}''_B = \dot{Q}''_{Ms,conv} \quad (13)$$

where $\dot{Q}''_{Ms,conv} = h_{conv,rs,i}(T_{M_s} - T_{rm})$ and $h_{conv,i}$ denotes the convection coefficient between the

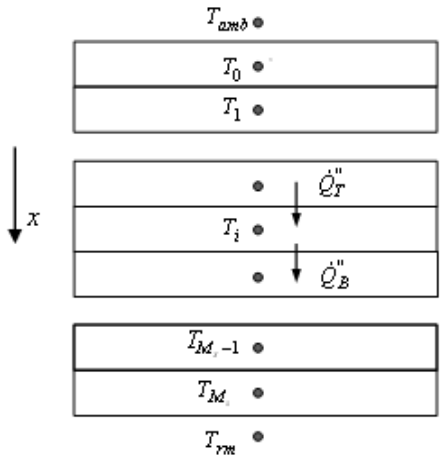

Figure 5: Section of the roof-slab with control volumes

inner slab surface and space room air. As will be shown in Section 4.1 $h_{conv,rs,i}$ may be calculated with the natural convection correlation given by equation (31).

Once the inner slab surface temperature is known the heat transmitted through the slab and subsequently transferred to the air may be calculated by

$$\dot{Q}_{rs,tr} = h_{conv,rs,i} A_{rs} \left(T_{Ms} - T_{rm}\right) \quad (14)$$

3.4 Heat gain through the window

The heat transferred through the window comprises conductive, convective and radiation heat transfer components. The conductive and convective heat transfer through the window is caused by the temperature difference between the indoor and outdoor air. The radiation heat transfer comprises shortwave solar radiation and long wave radiation heat exchange between the window and the environment. The total instantaneous heat gain through the window is calculated by

$$\dot{Q}_{hwd,tot,i} = \dot{Q}_{hwd,b} + \dot{Q}_{hwd,d} + \dot{Q}_{hwd,cond} \quad (15)$$

where $\dot{Q}_{hwd,b}$ denotes the heat transferred through the window due to beam shortwave radiation, $\dot{Q}_{hwd,d}$ heat transferred through the window due to diffuse radiation and $\dot{Q}_{hwd,cond}$ the heat transferred through the window due to conduction and convection. $\dot{Q}_{hwd,b}$ is calculated by (ASHRAE Fundamentals, 2005)

$$\dot{Q}_{hwd,b} = A_{wd} I_{solar,b} SHGC(\theta_{solar}) IAC \quad (16)$$

where A_{wd} is the window area, $I_{solar,b}$ the direct beam solar radiation incident on the window, $SHGC(\theta_{solar})$ the direct solar heat gain coefficient at the solar incident angle θ_{solar} and IAC the inside shading attenuation coefficient. The solar diffuse heat gain $\dot{Q}_{hwd,d}$ is calculated by

$$\dot{Q}_{hwd,d} = A_{wd} \left(I_{solar,d} + I_{solar,r}\right) SHGC(d) IAC \quad (17)$$

where $I_{solar,d}$ denotes the diffuse solar radiation, $I_{solar,r}$ the ground reflected solar radiation and $SHGC(d)$ the hemispherical average solar heat gain coefficient. The values utilized in this study for $I_{solar,b}$, $I_{solar,d}$, $I_{solar,r}$, $SHGC(\theta_{solar})$ and $SHGC(d)$ may be found in Appendix B. The conductive and convective heat gain through the window is calculated by

$$\dot{Q}_{hwd,cond} = U_{wd} A_{wd} \left(T_{amb} - T_{rm}\right) \quad (18)$$

where U_{wd} is the overall heat transfer coefficient that combines the center-of-glass *U*-factor, the edge-of-glass *U*-factor and the frame *U*-factor. U_{wd} incorporates the convective heat transfer between the air and the window as well as the conductive heat transfer through the window itself. *U*-factors for various window types may be found in ASHRAE Fundamentals 2005 (Chapter 31, Table 4). The *U*-factor utilized in this study was for a single glazing window with an aluminium frame and thermal breaks and had a *U*-factor of 5.43 W/m²K.

Only a fraction of the total instantaneous heat gain through the window $\dot{Q}_{hwd,tot,i}$ converts to an actual cooling load that results in an almost immediate change in the space air temperature. A large part of the window heat gain is radiant that only becomes a cooling load some time later. To take this time delay effect into account, ASHRAE recommends the use of a Radiant Time Series (RTS) procedure that utilises radiant time factors. The radiant time factors reflect the heat gain of earlier hours that becomes a cooling load in the current hour of operation.

The RTS procedure calculates cooling load based on the 24 hour heat gain profile of the specific heat source. The heat gain of each hour is split into radiant and convective parts. The convective part becomes an actual cooling load. Radiant time factors are applied to the radiant part of the current hour to account for the time delay from instantaneous heat gain to actual cooling load conversion. These factors are presented in Table 1.

ASHRAE Fundamentals 2005 (Chapter 30, Table 16) gives the convective portion of heat gain through a window with inside shade as 37%. The remaining 63% of the heat gain is radiant that would only become an actual cooling load sometime later. Thus

$$\dot{Q}_{hwd,conv} = 0.37 \dot{Q}_{hwd,tot,i} \quad (19)$$

and

$$\dot{Q}_{hwd,rad,i} = 0.63 \dot{Q}_{hwd,tot,i} \quad (20)$$

where $\dot{Q}_{hwd,rad,i}$ is the instantaneous radiant portion of the total window heat gain and $\dot{Q}_{hwd,conv}$ the convective portion of the total instantaneous window heat gain. If r_h denotes the radiant time factor for the *h*'th hour of the day then the actual cooling load of the radiant portion of the window

Table 1: The radiant time factors for non-solar heat gains for a building with medium weight construction, 10% glass and a carpet
(ASHRAE Fundamentals, 2005)

Hour	RTF (%)	Hour	RTF (%)	Hour	RTF (%)
0	46	8	1	16	1
1	18	9	1	17	1
2	10	10	1	18	1
3	6	11	1	19	0
4	4	12	1	20	0
5	2	13	1	21	0
6	2	14	1	22	0
7	1	15	1	23	0

heat gain for the *h*'th hour becomes

$$\dot{Q}_{hwd,rad} = r_0\dot{Q}_{hwd,rad,i} + r_1\dot{Q}_{h-1wd,rad,i} + r_2\dot{Q}_{h-2wd,rad,i} + r_3\dot{Q}_{h-3wd,rad,i} + \ldots + r_{23}\dot{Q}_{h-23wd,rad,i} \quad (21)$$

The actual window cooling load on the one-room building for hour *h* is the sum of the radiant and convective portions, i.e.

$$\dot{Q}_{hwd,tot} = \dot{Q}_{hwd,rad} + \dot{Q}_{hwd,conv} \quad (22)$$

3.5 Heat gain from lighting

Similar to the heat gain through the windows, the heat gain from lighting comprises a convective and radiant portion. The instantaneous lighting heat gain is calculated by

$$\dot{Q}_{hl,i} = \dot{q}_l A_{fl} Fu_l \quad (23)$$

where $\dot{q}_l$ is the instantaneous lighting load per floor area, A_{fl} the floor area and Fu_l the lighting usage factor. The convective portion of the lighting load constitutes 33% of $\dot{Q}_{hl,i}$ and the instantaneous radiant portion 67% (ASHRAE Fundamentals 2005, Chapter 30, Table 16). The actual cooling load of the instantaneous radiant portion may be calculated by applying the RTS factors (see Table 1) similar to equation (21). The total cooling load from lighting is calculated as the sum of the convective and radiant portions similar to that of equation (22).

3.6 Heat gain from people and office equipment

The remaining heat gains to the one-room building are that of people, equipment and heat transmission through the floor. Similar to the lighting and window heat gains , the heat gains from people may yet again be broken up into a convective and radiative portion. The actual cooling load of people occupying the one-room building becomes

$$\dot{Q}_{hp,tot} = \dot{Q}_{hp,rad} + \dot{Q}_{hp,conv} \quad (24)$$

where $\dot{Q}_{hp,rad}$ gives the radiative portion of the people load and $\dot{Q}_{hp,conv}$ the convective portion. According to ASHRAE Fundamentals 2005 (Chapter 30, Table 1) the radiant portion of the heat gain from a person performing moderate office work is 58% and the convective portion is 42%, thus

$$\dot{Q}_{hp,conv} = 0.42\dot{Q}_{hp,tot,i} = 0.42N_P Fpo\dot{q}_{p,i} \quad (25)$$

where $\dot{Q}_{hp,tot,i}$ is the total instantaneous heat release from people, N_p is the number of people in the one-room building, Fpo the people occupancy factor and $\dot{q}_{p,i}$ the instantaneous sensible heat gain from a person performing office work. Hence the instantaneous radiant heat gain becomes

$$\dot{Q}_{hp,rad,i} = 0.58\dot{Q}_{hp,tot} = 0.58N_p Fpo\dot{q}_{p,i} \quad (26)$$

To calculate $\dot{Q}_{hp,rad}$ the RTS factors are applied to $\dot{Q}_{hp,rad,i}$ in a similar fashion as that of the window loads, see equation (21).

The office equipment in the one-room building is assumed to be a computer and accompanying monitor. The heat gain from a typical computer and monitor may be obtained from ASHRAE Fundamentals 2005 (Chapter 30, Table 8). According to ASHRAE Fundamentals (2005), the heat gain through the floor may be regarded as negligible when cooling load calculations are performed. The heat gain through the floor of the one-room building is therefore assumed zero and is thus not included in the mathematical model.

4. Modeling of the sustainable energy cooling alternatives

In the previous section the mathematical model for calculating the base case cooling load of the one-room building have been derived. In this section the mathematical model is presented where each of the sustainable cooling alternatives is integrated into the one-room building separately.

4.1 Night flushing

When night flushing is applied to the one-room building, the equations for the base case cooling load as derived in Section 3 applies. The major difference between the night flushing and the base case is the high volume at which ambient air is flushed through the building at night time. When cold ambient air is admitted to the one-room building, the thermal energy in the building structure is reduced by means of convection heat transfer from the wall, roof-slab and floor surfaces. When the building has lower thermal energy the peak room temperature would be lower since less energy is transferred to the room air the following day.

Night flushing not only cools the air in the room but also removes stored energy from the walls and roof-slab. The rate at which energy is removed from the building structure depends greatly on the convective heat transfer coefficient. Pfafferott et al. (2003) report that accurate modeling of the

convective heat transfer coefficients are essential in simulating the effect of night flushing of a building. This notion is further supported by Artmann et al. (2008) as well as Blondeau et al. (1997). According to Dascalaki et al. (1994) both natural and forced convection are the primary mechanisms of heat transfer inside buildings. Both natural and forced convection effects are comparable when (Cengel and Boles, 2002)

$$\frac{Gr_L}{Re_L^2} \approx 1 \tag{27}$$

where Gr_L is the Grashof number, Re_L the Reynolds number and L characteristic length defined as surface area divided by the surface perimeter. When the term on the left hand side of equation (27) is significantly smaller than 1, free convection is negligible and when significantly larger than 1, forced convection becomes negligible. When Gr_L and the Re_L are calculated for a typical wall temperature of 21 °C, a room air temperature of 12 °C and a wall length of 3 m equation (27) becomes

$$\frac{1.015}{u_0^2} = 1.0 \tag{28}$$

where u_0 denotes the air velocity within the one-room building which may be approximated by the volumetric flow rate divided by the average room surface are

$$u_0 = \frac{V_{build}\, ACH}{10800}\left(\frac{1}{w_{build}\, h_{build}} + \frac{1}{l_{build}\, w_{build}} + \frac{1}{h_{build}\, l_{build}}\right) \tag{29}$$

where V_{build} denotes the volume of the air in the one-room building, ACH the air changes per hour, w_{build} the width of the one-room building, h_{build} the height of the one-room building and l_{build} the length of the one-room building. From equation (28) the air flow velocity must be in the order of 1 m/s for forced convection to be comparable with natural ventilation. For the one-room building dimensions given in Figure 1 this means that the building night flush rate needs to be in the order of 720 ACH for forced convection to be significant.

Both Artmann et al. (2008) and Geros et al. (1999) found that increasing the air changes rate beyond 32 ACH does not significantly decrease the peak room temperature the following day. Since this air change rate is significantly less than the 720 ACH required for forced convection to take place, the heat transfer coefficient for the inside wall surfaces when the building is flushed, will be calculated from natural convection correlations. This agrees with Blondeau et al. (1997) who made the assumption of still air values for the heat transfer convective coefficients when a building is highly ventilated. This approach is however in contrast to Chandra and Kerestecioglu's (1984) proposal to double the Clark (1989) proposal of quadrupling the internal convection heat transfer coefficient when a room is highly ventilated.

Pfafferott et al. (2003) utilised natural ventilation correlations by Alamdari and Hammond as well as Khalifa and Marshall to determine the convective heat transfer coefficients. These heat transfer coefficients can be found in Dascalaki et al. (1994). In this study the Churchill and Chu (Cengel and Boles, 2002) natural convection correlations are used for the vertical surfaces of the walls

$$\overline{Nu}_L = \frac{h_{conv,i} L}{k_{rm,a}} = \left[0.825 + \frac{0.387 Ra_L^{1/6}}{\left[1 + (0.492/Pr)^{9/16}\right]^{8/27}}\right]^2 \tag{30}$$

where $\overline{Nu}_L$ denotes the average Nusselt number, Ra_L is the Rayleigh number, L the width of the wall surface and $k_{rm,a}$ the thermal conductivity of the air in the room. Equation (30) has no restrictions and is valid for $0 < Ra_L < \infty$. For the slab in contact with the air in the room the correlation proposed by Incorpera and DeWitt (2002) for a lower surface of a cooled plate will be used, i.e.

$$\overline{Nu}_L = \frac{h_{conv,i} L}{k_{rm,a}} = 0.15 Ra_L^{1/3} \tag{31}$$

4.2 Active mass cooling

The structural mass of the one-room building may be cooled by circulating water in a pipe network embedded within the roof-slab. The cool water may be obtained from a cooling tower or even a roof-pond or roof-spray system. Buildings situated close to the coast may employ the sea for such a cold water source. The layout geometry of the water pipes, the spacing between the pipes and the dimensions of the concrete slab are essential design parameters for this type of system (Koschenz et al. 1996). Figure 6 depicts the centre control volume of the roof-slab with the embedded pipes.

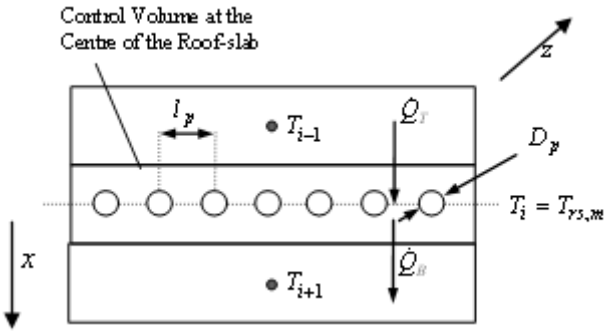

Figure 6: Control volume at the centre of the slab with embedded pipes in which the water circulates

According to Koschenz and Dorer (1999) it is reasonable to assume a mean temperature within the slab at the pipe level with a resistance coefficient $R_{w,rs}$ that exists between the water temperature T_w and the mean slab temperature $T_{rs,m}$. The heat transfer coefficient $R_{w,rs}$ is dependent on the diameter of the pipes and the spacing of the pipes. According to Koschenz and Dorer (1999) when $l_p = 0.2\,\text{m}$ and $D_p = 0.03\,\text{m}$ $R_{w,rs}$ has a value of 0.05 W/m²K/W. Other values for $R_{w,rs}$ corresponding to different pipe diameters and spacing may be found in Koschenz and Dorer (1999).

The heat transfer in the slab may also be assumed one dimensional (Koschenz and Dorer, 1999). For the interior control volume where the pipe network is located the temperature may be calculated by

$$T_i^{t+\Delta t} = T_i + \frac{\Delta t}{\Delta x \rho_{rs} C_{rs}} \left(\dot{Q}_T'' + \dot{Q}_w'' - \dot{Q}_B'' \right) \tag{32}$$

where $\dot{Q}_T''$ is calculated using equations (12) and $\dot{Q}_B''$ from equation (13). The heat transfer from the water in the pipe network and the center control volume may be calculated by

$$\dot{Q}_w'' = \frac{T_w - T_{rs,m}}{R_{w,rs}} \tag{33}$$

where $T_{rs,m}$ denotes a temperature at a plane located at the centre of the embedded pipes, T_w the water temperature and $R_{w,rs}$ the resistance coefficient. The temperatures of the remaining control volumes in the roof-slab are similarly calculated to that of the base case mathematical model.

Another consideration is the variation in water temperature as it flows through the embedded pipes of the roof-slab. Koschenz and Dorer (1999) propose that a single average water temperature be used in the pipes and that this temperature be approximated by using a logarithmic average. As an alternative, discretizing the slab in the *z*-direction is also proposed. In this study the variation in water temperature will be modeled by dividing the slab into control volumes along the route of the embedded pipes. It can be shown by means of an energy balance that the temperature of the water flowing out of each control volume $T_{w,o}$ may be approximated in terms of the inlet temperature $T_{w,i}$

$$T_{w,o} = \frac{T_{w,i}\left(R_{w,rs}\dot{m}_w C_p - A_{cv}\right) + A_{cv} T_{rs,m}}{R_{w,rs}\dot{m}_w C_p} \tag{34}$$

where $\dot{m}_w$ denotes the water mass flowrate, C_p the specific heat of water at a constant pressure and A_{cv} the area of the control volume through which the heat flows.

4.3 Roof-spray cooling

The basic concept of roof-spray cooling is to continuously wet the roof surface by cooling it down with sprayed water (Carrasco et al. 1987). With a wetted roof more heat from the roof surface is lost to the atmosphere due to evaporation resulting in a reduction in roof temperature and heat entry to the building (Jain, 2006). Figure 7 shows the outer control volume at the 0th node of the wetted roof surface.

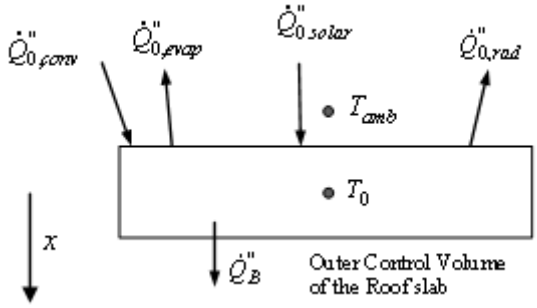

Figure 7: Control volume of the wetted roof in contact with the ambient

In the derivation of the mathematical model of the roof-spray system Jain (2006), Clements and Sherif (1998) as well as Carrasco et al. (1987) assumes a negligible thickness of the wetted water layer on the roof surface. The reasoning behind this was that the sprayed water on the roof adds a constant evaporative heat flux to the roof control surface without affecting the convective heat transfer (Carrasco et al. 1987). The temperature of the outer control volume may be expressed explicitly by equation (11). For the case of the roof-spray $\dot{Q}_T''$ is calculated by

$$\dot{Q}_T'' = \dot{Q}''_{0.solar} - \dot{Q}''_{0,rad} + \dot{Q}''_{0,conv} - \dot{Q}''_{0,evap} \tag{35}$$

where the terms $\dot{Q}''_{0.solar}$, $\dot{Q}''_{0,rad}$ and $\dot{Q}''_{0,conv}$ may be calculated similarly to the base case model. At the wetted surface water vapour diffuses into the ambient air as a result of Fick's law of diffusion. This evaporative heat flux may be calculated by (Tiwari et al. 1981)

$$\dot{Q}''_{0,evap} = A h_{evap} (p_{vap,rs} - \phi_{amb} p_{vap,amb}) \tag{36}$$

where A is a constant value of 0.013 that incorporates the latent heat of vapourisation, specific heat of air at constant pressure, the density of air , the mass transfer coefficient, the air pressure, the mass of air and that of the water vapour. h_{evap} in equation (36) denotes the heat transfer coefficient between the water surface and the ambient air, ϕ_{amb} the relative humidity of the air, $p_{vap,rs}$ the partial pressure of the water vapour evaluated at the weited roof surface temperature, and $p_{vap,amb}$ is the partial vapour pressure of the ambient air.

$\dot{Q}_B''$ in Figure 7 may be calculated from equation (13) and the heat transmitted through the slab and transferred to the air from equation (14).

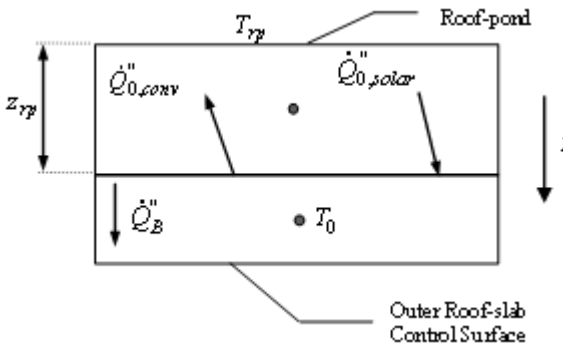

Figure 8: Outer upper control of the roof and the roof-pond as a single control volume

4.4 Roof-pond cooling

The roof-pond comprises a pond of water on the roof surface that reduces the heat entering the one-room building. Figure 8 depicts the outer control volume at the 0th node of the roof and the roof-pond as a single control volume of thickness z_{rp}.

Similar to the base case model the temperature of the outer control volume may be expressed by equation (11). However, with the inclusion of the roof-pond $\dot{Q}''_T$ is calculated by

$$\dot{Q}''_T = \dot{Q}''_{0,solar} - \dot{Q}''_{0,conv} \quad (37)$$

where $\dot{Q}''_{0,solar} = I_{solar,tot}\alpha_{rs,rp}$, $\dot{Q}''_{0,conv} = h_{rs,w}(T_0 - T_{rp})$ and $I_{solar,tot}$ denotes the incident solar shortwave radiation onto the roof surface, $\alpha_{rs,rp}$ the portion of solar radiation absorbed by the roof-slab, T_{rp} the roof-pond temperature and $h_{rs,w}$ the convective heat transfer coefficient between the roof surface and the roof-pond. $\alpha_{rs,rp}$ is a function of the roof reflectivity $\rho_{r,rs}$, the water reflectivity $\rho_{r,w}$, the water transmissivity τ_w, and the roof surface solar absorbtivity α_{rs}. It can be shown that $\alpha_{rs,rp}$ may be calculated by

$$\alpha_{rs,rp} = \frac{\tau_w \alpha_{rs}}{1 - \rho_{r,rs}\rho_{r,w}} \quad (38)$$

Both Sodha et al. (1980:2) and Jain (2006) uses a value of 135 W/m²K for the heat transfer coefficient $h_{rs,w}$ between the roof surface and the roof-pond. However, under stagnant conditions the heat transfer between the roof surface and the roof-pond would be natural and natural convection correlations may be employed (Mills, 2000).

The roof-pond temperature may be calculated by

$$T_{rp}^{new} = T_{rp}^{old} + \frac{\Delta t}{m_{rp}C_p}\left(\dot{Q}_{solar} - \dot{Q}_{sky} - \dot{Q}_{0,conv} - \dot{Q}_{rp,conv} + h_g\dot{m}_{rp,cond} - h_g\dot{m}_{rp,evap}\right) \quad (39)$$

where $\dot{Q}_{sky} = \varepsilon_{rp}\sigma A_{rp}(T_{rp}^4 - T_{sky}^4)$, $\dot{Q}_{0,conv} = h_{rs,w}A_{rp}(T_{rp} - T_0)$, $\dot{Q}_{solar} = \alpha_{s,rp}A_{rp}I_{solar}$, $\dot{Q}_{rp,conv} = h_{rp,amb}A_{rp}(T_{rp} - T_{amb})$, A_{rp} the surface area of the roof-pond, ε_{rp} the roof-pond emissivity, h_g denotes the enthalpy of the vapour in the ambient air, $\dot{m}_{rp,cond}$ the rate of condensation, $\dot{m}_{rp,evap}$ the rate of evaporation, $\alpha_{s,rp}$ the roof-pond solar absorptivity and $h_{rp,amb}$ the convection heat transfer coefficient between the roof-pond water and the ambient air. Condensation and evaporation does not occur simultaneously and in all cases either $\dot{m}_{rp,cond}$ or $\dot{m}_{rp,evap}$ will be zero. Correlations for the calculation of $\dot{m}_{rp,cond}$ and $\dot{m}_{rp,evap}$ may be found in Mills (2000). $h_{rp,amb}$ may be calculated using equation (8).

5. Discussion of computer simulated results

The mathematical model of the one-room building for the base case and the cases where the sustainable cooling alternatives are included were used in a computer program to simulate the room temperature and the required cooling load of the one-room building for a typical summer clear sky day in Stellenbosch. The input variables as well as meteorological conditions used in the computer simulations are presented in Appendix B.

At the start of the simulations an initial roof-slab and wall temperature of 27 °C was assumed. The initial room temperature was taken as 22 °C, while an initial roof-spray temperature of 24 °C and an initial roof-pond temperature of 15 °C was assumed. The computer simulation was repeated for 3 days, after which convergence had been found to have achieved.

5.1 Room temperature and cooling load profile of the one-room building with the sustainable cooling methods included separately

The room temperature and cooling load profile of the one-room building for the base case, night flushing, roof-spray, roof-pond and active mass cooling are depicted in Figure 9 and Figure 10. The cooling load profile was generated for a room thermostat setting of 22 °C. The night flushing technique was activated during nocturnal hours between 24:00 and 07:00 at a rate of 32 ACH. For the roof-pond simulation, the roof-pond water level was set equal to 100 mm. With the active mass cooling option, water was continuously circulated through a pipe network embedded in the roof-slab at a rate of 1 kg/s and an initial temperature of 15 °C.

Figure 9 shows that the room temperature profile coincides well with the cooling load profile depicted in Figure 10 since the peaks and valleys occur at the same point in time. From Figure 10 the peak room temperature is seen to be 1.83 °C lower than the peak ambient temperature and occurs at a delay of 7 hours. Mull (1998) reports that the thermal mass of a building directly affects the time lag between the peak instantaneous heat gain and the peak cooling load. Although not shown here, the peak instantaneous heat gain occurs at approxi-

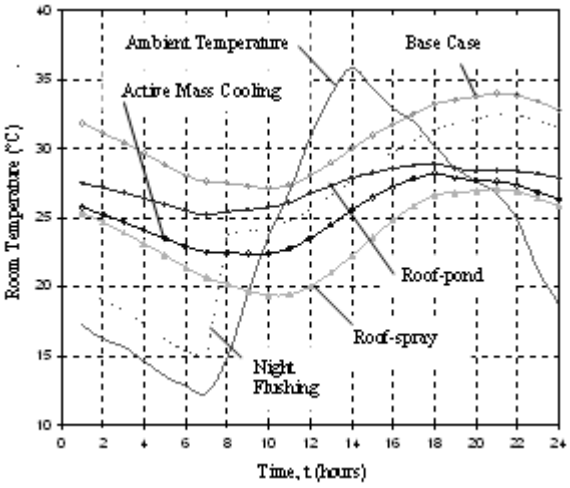

Figure 9: Room temperature profile of the one-room building with the sustainable cooling alternatives included separately

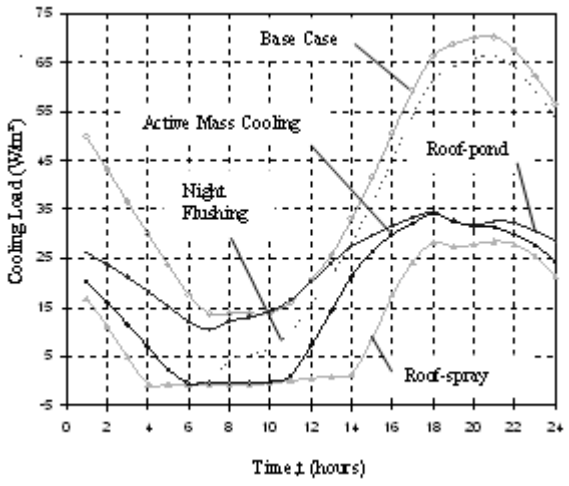

Figure 10: Cooling load profile of the one-room building with the sustainable cooling alternatives included separately

mately the same time as the peak ambient temperature. The greater the thermal mass of a building and the larger the time lag, the lower the peak cooling load (Mull, 1998). Since the one-room building has a high thermal mass (building weight above 1000 kg/m^2) it is understandable that the peak cooling load and room temperature lags the peak ambient air by 7 hours.

The peak room temperature reduction of 1.53 °C (33.97 °C to 32.45 °C, see Figure 9) by the night flushing technique agrees well with the temperature reductions of 1 to 3 °C found by Kolokotroni *et al.* (1998). Both Artmann *et al.* (2008) and Kolokotroni *et al.* (1998) pointed out that the room temperature reduction provided by night flushing is highly dependent on the air change rate, the thermal mass of the building, heat gains and meteorological conditions. The peak room temperature for higher air change rates is also expected not to decrease since the night flushing simulation was conducted with an air change rate of 32 ACH. (12 ACH higher than the critical air change rate of 20 ACH reported by Artmann *et al*. (2008).

The application of the roof-spray showed a peak room temperature reduction of 6.9 °C (33.97 °C to 27 °C, see Figure 9) while active mass cooling produced a peak room temperature reduction of 6.4 °C (33.97 °C to 27.62 °C, refer to Figure 9). Both the roof-spray and active mass cooling showed a temperature profile similar to that of the base case but at an average offset of 7.1 °C for the roof-spray and 5.33 °C for active mass cooling. The roof-pond reduced the peak room temperature by 5.6 °C (33.97 °C to 28.41 °C) with an average temperature reduction of 3.33 °C over the 24 hour time period.

Table 2 gives the peak cooling load *** over a 24 hour period with the corresponding peak cooling load percentage reduction for each of the sustainable cooling alternatives. Table 3 gives the total heat energy transferred to the one-room building over a 24 hour period $E_{rm,tot}$ and the percentage reduction corresponding to each of the sustainable cooling alternative options. These tables were generated for a 22 °C temperature setting. The total energy supplied corresponds thus to the additional heat that must be removed by the active cooling system for the given temperature setting.

Table 2: Peak cooling load of the one-room building with the sustainable cooling alternatives included separately

Sustainable cooling alternative method	*Peak cooling load* $\dot{q}_{pk,tot}$ *(W/m²)*	*% Reduction in peak cooling load (W/m²)*
Base case	70.25	0%
Roof-spray	28.55	59.36%
Roof-pond	34.38	51.07%
Active mass cooling	34.15	51.39%
Night flushing	66.39	5.50%

Table 3: Total heat energy transferred to the one-room building with the sustainable cooling alternatives included separately

Sustainable cooling alternative	*Total energy transferred* $E_{rm,tot}$ *(kJ/m²)*	*% reduction in net energy transferred* $E_{rm,tot}$
Erm,tot		
Base case	3469.09	0%
Roof-spray	963.09	72.24%
Roof-pond	2059.91	40.62%
Active mass cooling	1436.86	58.58%
Night flushing	2370.59	31.67%

Under base case conditions the peak room cooling load for the one-room building is 70 W/m^2. Night flushing reduced the peak cooling load by the smallest amount since this option could only reduce the peak cooling load by 3.9 W/m^2. The roof-spray option produced the highest reduction in peak cooling load by providing 42 W/m^2 of cooling.

Comparing the peak cooling load reduction of the various sustainable cooling alternatives it can be seen from Table 2 that the roof-spray system reduced the peak cooling load the most, i.e. by 59.36%. This is significantly more than the 25% cooling load reduction reported by Holder (1957) and Thappen (1943). The discrepancy may be ascribed to the different building configuration and weather conditions under which Holder (1957) and Thappen (1943) performed their tests. The 51.07% peak load reduction obtained from the roof-pond system is approximately 21% more than the 30% reported by Kharrufa and Adil (2006). The difference in cooling load reduction obtained may be ascribed to the 26 °C temperature setting Kharrufa and Adil used in their calculations.

The roof-spray system also showed the largest reduction in net energy transfer to the one-room building over the 24 hour period. Under base case conditions the net energy transferred to the one-room building was 3469.1 kJ/m^2. With the inclusion of the roof-spray system the net energy was reduced to 963.1 kJ/m^2 and which corresponds to a 72% reduction. The energy reduction by the roof-spray was significantly more than that obtained from active mass cooling, night flushing and the roof-pond system.

5.2 Room temperature and cooling load profile of the one-room building in conjunction with various combinations of the sustainable cooling methods

Figure 11 gives the room temperature and Figure 12 the cooling load profile of the one-room building for the following combinations of the sustainable cooling alternative options:

i. Roof-spray and night flushing
ii. Roof-pond and night flushing
iii. Active mass cooling and night flushing
iv. Active mass cooling, roof-pond and night flushing

Figure 11 shows that the combination of roof-spray and night flushing reduced the peak room temperature from the base case by 7.9 °C. The combination of roof-pond and night flushing gave a 6.5 °C peak room temperature reduction while the combination of active mass cooling and night flushing yielded a 7 °C peak room temperature reduction. This compares favourably to the case where the roof-spray, roof-pond and active mass cooling systems were employed as stand-alone systems since the addition of night flushing to these sustainable cooling options produced an additional temperature reduction in the order of 0.7 °C to 1 °C. The combination of active mass cooling, night flushing and roof-pond showed the best energy saving potential by reducing the peak room temperature 7.2 °C.

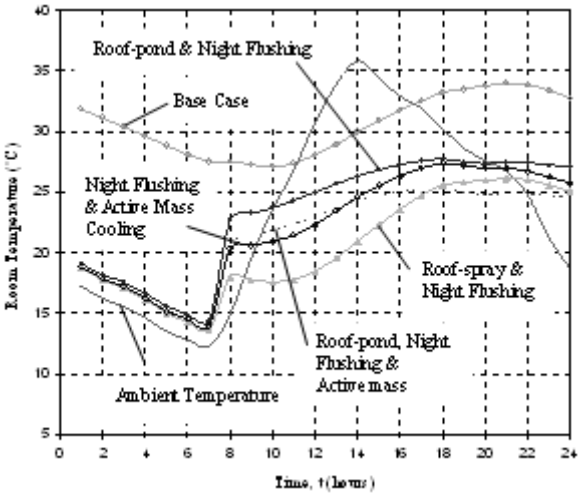

Figure 11: Room temperature profile of the one-room building with the sustainable cooling alternatives included in combinations

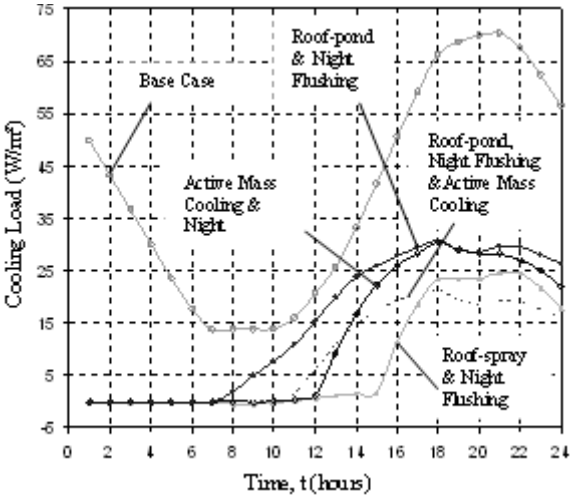

Figure 12: Cooling load profile of the one-room building with the sustainable cooling alternatives included in combinations

Table 4 gives the peak cooling load $\dot{q}_{pk,tot}$ obtained over a 24 hour period with the corresponding peak cooling load percentage reduction for the combinations of the sustainable cooling alternatives. Table 5 gives the total heat energy transferred to the one-room building over a 24 hour period $E_{rm,tot}$ as well as the percentage reduction corresponding to the combinations of the sustainable cooling alternative.

Table 4 shows that the combination of roof-spray and night flushing reduced the peak cooling load from the base case value to 24.53 W/m^2. The

combination of roof-pond and night flushing reduced the peak cooling load to 30.7 W/m^2 while the combination of active mass cooling and night flushing reduced the peak cooling load to 30.30 W/m^2. By comparing Table 2 with Table 4 it can be seen that the inclusion of night flushing with the roof-pond, roof-spray and active mass cooling options an additional reduction in the order of 5 to 6% of the peak cooling load could be achieved. The best results were obtained for a combination of the roof-pond, active mass cooling and night flushing. The one-room building peak cooling load was lowered from 70 W/m^2 to 21.4 W/m^2 which corresponds to a 70% reduction in peak cooling load.

Table 4: Peak cooling load of the one-room building with the sustainable cooling alternatives included in combinations

Sustainable cooling alternative method	*Peak cooling load* $\dot{q}_{pk,tot}$ *(W/m^2)*	*% Reduction in peak cooling load* $\dot{q}_{pk,tot}$ *(W/m^2)*
Base case	70.25	0%
Roof-spray & night flushing	24.53	65.08%
Roof-pond & night flushing	30.68	56.33%
Active mass cooling & night flushing	30.30	56.87%
Active mass cooling, roof-pond & night flushing	21.41	69.52%

Table 5: Total heat energy transferred to the one-room building with the sustainable cooling alternatives included in combinations

Sustainable cooling alternative	*Total energy transferred* $E_{rm,tot}$ *(kJ/m^2)*	*% reduction in net energy transferred* $E_{rm,tot}$ *(kJ/m^2)*
Base case	3469.09	0%
Roof-spray & night flushing	685.11	80.25%
Roof-pond & night flushing	1324.24	61.83%
Active mass cooling & night flushing	1050.25	69.73%
Active mass cooling, roof-pond & night flushing	795.01	77.08%

The net energy transferred to the one-room building air in the 24 hour period was also significantly decreased by the addition of night flushing to the sustainable cooling alternatives. In all cases, the total energy transferred to the one-room building air could be reduced by more than 60% from the base case value. The greatest reduction was found by the combination of roof-spray and night flushing where the net energy transferred to the one-room building was reduced by 80.2%.

It can be concluded that the large temperature and cooling load reduction produced by the combination of night flushing and a roof-spray as well as the combination of the roof-pond, active mass cooling and night flushing should be sufficient to maintain temperature within comfort levels for a building where the required cooling load does not exceed 25 W/m^2.

6. Conclusion and recommendation

A one-room building was assumed such that the cooling ability of night flushing, active mass cooling, roof-spray and the roof-pond system could be investigated and compared to the same reference and input conditions. All the sustainable cooling alternative options proved to decrease the cooling load required to maintain the one-room building at a constant temperature for the 24 hour operation period. The most important reduction occurred at the peak of the cooling load profile as this not only constituted a saving in the energy consumed by a conventional air conditioner but also decreased the required size of the air conditioner.

Active mass cooling, roof-pond and night flushing are viable options that may be employed with confidence to lower the heat gain of buildings. The amount by which the peak cooling load can be reduced with each sustainable cooling alternative depends on variables such as the building structure, the orientation, location, etc. With the application of the roof-pond and active mass cooling systems to the one-room building configuration, peak cooling load reductions in the order of 50% could be achieved. Night flushing as a stand-alone system was not that effective and only yielded a peak cooling load reduction in the order of 6%. For the given peak cooling load of 70.25 W/m^2 and the high ambient temperatures under which the simulations were performed, the active mass cooling and roof-pond system was able to lower the room temperature below 26 °C for the morning hours of the day. However, around the afternoon hours the room temperature raised to approximately 28 °C for the active mass cooling system and 27 °C for the roof-spray.

The roof-spray system showed the best result since the peak cooling load could be reduced by almost 60%. The corresponding peak room temperature reduced by approximately 6.9 °C (from 33.97 °C to 27.04 °C). In the morning hours of the day the roof-spray system could lower the room temperature well below the desired set-point of 22 °C. This result is favourable in the sense that in milder climate conditions the necessity of a conventional air conditioner may be averted. An addition-

al measure that can be taken to boost the cooling ability of the roof-pond, roof-spray and active mass cooling is to combine these sustainable cooling alternative options with the night flushing technique. By doing this an additional reduction of 5 to 6% in the peak cooling load can be expected.

Over a daily cycle night flushing, active mass cooling and the roof-pond system produces net energy savings of 32%, 41% and 59% respectively. The roof-spray system would give energy savings on the region of 70%. It must, however, be taken into account that the installation of any of the sustainable cooling alternatives may only be possible if the building design permits it. Installation of any of the cooling alternatives may be impeded by physical constraints such as water availability, building thermal mass or an insufficient area on which a roof-pond may be built.

One aspect that should be considered when designing a roof-pond and roof-spray system for a building is water consumption. At locations where water is abundantly available the implementation of these systems should not be problematic. However, in water scarcity areas the implementation of a roof-pond and roof-spray would have to be considered more carefully as the water would have to be treated as a sustainable resource.

It is recommended that a cost analysis be performed such that the payback period may be calculated for each sustainable cooling alternative option. The payback period would reveal if it is economically feasible to include each of the sustainable cooling alternatives in the construction of a building. It should be pointed out that the cooling loads refer to the thermal energy only and thus do not include the electrical pumping load requirements. It is further recommended that the sustainable cooling alternatives be analysed experimentally by applying them to a full scale building of which the room temperature is continuously monitored. The theoretically determined cooling load and room temperature of the building can then be compared with the experimental results to provide further insight into the validity of the mathematical model as derived in this paper.

Nomenclature

A Area (m^2)
C Constant Specific Heat (J/kgK)
D Diameter (m)
E Energy (J)
Fpo People Occupancy Factor
Fu Usage Factor
Gr Grashof Number $Gr = \left(\frac{g\beta(T_s - T_{amb})L^3}{\nu^2} \right)^2$
h Heat Transfer Convection Coefficient (W/m^2K), Enthalpy (J/kgK) or Height (m)
I Incident Solar Radiation (W/m^2)
k Thermal Conductivity (W/mK)
l Length (m)
L Characteristic Length (m)
m Mass (kg)
$\dot{m}$ Mass Flowrate (kg/s)
N Number
Nu Nusselt Number
p Pressure (Pa)
Pr Prandtl Number ($Pr = \nu / \alpha$)
$\dot{q}$ Rate of Heat Transfer per Unit Area (W/m^2)
$\dot{Q}$ Rate of Heat Transfer (W/m^2)
$\dot{Q}''$ Rate of Heat Transfer per square area (W/m^2)
r Radiant Time Factor
R Thermal Resistance (W/K) or Resistance Coefficient (W/m^2K)
Re Reynolds Number ($Re = uL / \nu$)
t Time (s) or Thickness (mm)
T Temperature (K or °C)
u Velocity (m/s)
U Overall Heat Transfer Coefficient (W/m^2K)
$\dot{V}$ Volume Flow rate (m^3/s)
V Volume (m^3)
w Width (m)
x Distance (m)
z Depth (m)

Variables

Greek symbols

α Absorptivity or Thermal Diffusivity ($\alpha = k / C_\rho$), (m^2/s)
β Volume Thermal Expansion Coefficient, K^{-1}
Δ Differential
ϑ Partial Derivative
ε Emissivity
μ Dynamic Viscosity (m/kgs)
ν Kinematic Viscosity ($\nu = \mu / \rho$), (m^2/s)
ρ Density (kg/m^3) or Reflectivity
σ Stefan-Boltzmann constant ($5.67 \times 10^{-8} W/m^2k^4$)
τ Transmissivity
φ Humidity (%)
ϖ H

Sub- and superscripts

a Air
amb Ambient
b Beam
build Building
B Bottom
cond Conduction

conv	Convection
cv	Control Volume
d	Diffuse
e	Equipment
evap	Evaporation
fl	Floor
g	Gas
h	Heat or Hour
i	Node index, In, Inner or Instantaneous
if	Infiltration
l	Lighting
L	Characteristic Length, Left
m	Mean
M	number of control volumes in the wall
new	New
o	Out or Outer
old	Old
p	Pressure, People or Pipes
pk	Peak
r	Reflectivity
rad	Radiation
rm	Room
rp	Roof-pond
rs	Roof-slab
R	Right
s	Surface or Slab
sbw	Single Brick Wall
sky	Sky
solar	Solar
t	temperature
tot	Total
tr	Transmission
T	Top
vap	Vapour
w	Water
wd	Window
wl	Wall

Abbreviations

ACH	Air Changes per Hour (#)
ACPD	Air Changes per Day (#)
IAC	Inside Shading Attenuation Coefficient
NF	Night Flushing
RP	Roof-pond
RTS	Radiant Time Series

Appendix A

The following questions were asked in the sample

1) Indicate your occupation by ticking in the relevant box below.

☐ Student ☐ Architect/Quantity Surveyor
☐ Engineer / Technologist ☐ Involved at tertiary institution
☐ Building Developer ☐ Financial involvement
☐ Designer ☐ Contractor / Builder
☐ Project Manager ☐ Other

2) Indicate the three most well known sustainable cooling alternative methods.

1) Indicate your occupation by ticking in the relevant box below.
☐ Student ☐ Architect/Quantity Surveyor
☐ Engineer / Technologist ☐ Involved at tertiary institution
☐ Building Developer ☐ Financial involvement
☐ Designer ☐ Contractor / Builder
☐ Project Manager ☐ Other

2) Indicate the three most well known sustainable cooling alternative methods.

☐ Active Mass Cooling ☐ Night Sky Radiative Cooling
☐ Phase Change Materials ☐ Adsorption Cooling
☐ Evaporative Cooling with Chimney ☐ Thermal Chimney for Natural Ventilation
☐ Night Flushing/Purging ☐ Earth Cooling Tubes with water/air
☐ The options provided above are unfamiliar to me

3) Based on your experience, which three of the following sustainable cooling alternatives could work?

☐ Active Mass Cooling ☐ Night Sky Radiative Cooling
☐ Phase Change Materials ☐ Adsorption Cooling
☐ Evaporative Cooling with Chimney ☐ Thermal Chimney with for Natural Ventilation
☐ Night Flushing/Purging ☐ Earth Cooling Tubes with water/air cooling
☐ None of the above

4) Which of the following sustainable cooling alternatives have been implemented the most?

☐ Active Mass Cooling ☐ Night Sky Radiative Cooling
☐ Phase Change Materials ☐ Adsorption Cooling
☐ Evaporative Cooling with Chimney ☐ Thermal Chimney for Natural Ventilation
☐ Night Flushing/Purging ☐ Earth Cooling Tubes with water/air
☐ I am not sure

5) What would be the two most attractive benefits of these sustainable cooling alternatives?

☐ CO2 Emission Reduction ☐ Building Running Cost Reduction
☐ Better Building Energy Efficiency ☐ Green Building "Image"
☐ Small scale contribution to lower global warming ☐ Shifting the mindsets of the relevant stakeholders

6) Which two sustainable cooling alternatives address the two selected benefits the best?

☐ Active Mass Cooling ☐ Night Sky Radiative Cooling
☐ Phase Change Materials ☐ Adsorption Cooling
☐ Evaporative Cooling with Chimney ☐ Thermal Chimney for Natural Ventilation
☐ Night Flushing/Purging ☐ Earth Cooling Tubes with water/air
☐ I am not sure

7) Should a financial analysis show that the payback period for all the sustainable alternatives ranges from 3 to 5 years, which sustainable cooling alternatives would you install in a building?

☐ Active Mass Cooling ☐ Night Sky Radiative Cooling
☐ Phase Change Materials ☐ Adsorption Cooling

☐ Evaporative Cooling with Chimney
☐ Thermal Chimney for Natural Ventilation
☐ Night Flushing/Purging
☐ Earth Cooling Tubes with water/air

8) Which of the following sustainable cooling alternatives would attract the greatest amount of funds for investment?

☐ Active Mass Cooling
☐ Night Sky Radiative Cooling
☐ Phase Change Materials
☐ Adsorption Cooling
☐ Evaporative Cooling with Chimney
☐ Thermal Chimney for Natural Ventilation
☐ Night Flushing/Purging
☐ Earth Cooling Tubes with water/air
☐ None of the above

Appendix B

The input parameters employed in the One-Room Building are given in table A.1.

Table A.1: Input parameters for the base case simulation of the one-room building

Description	*Symbol*	*Units*	*Value*
Building Dimensions			
Width	w_{build}	m	6
Length	l_{build}	m	6
Height	h_{build}	m	3
Wall thickness (brick)	t_{wl}	mm	230
Roof-slab thickness (concrete)	t_{rs}	mm	200
Window (North Facing)			
Width	w_{wd}	mm	1200
Height	h_{wd}	mm	1000
Window thickness	t_{wd}	mm	6
Internal Shading Coefficient	IAC	-	0.68
Overall Convection Heat Transfer Coefficient	U_{wd}	W/m²K	5.24
Building Properties			
Wall thermal conductivity	k_{sbw}	W/mK	0.72
Wall density	ρ_{sbw}	kg/m³	1920
Specific heat	C_{sbw}	J/kgK	835
Roof-slab thermal conductivity	k_{rs}	W/mK	1.1
Roof-slab density	ρ_{rs}	kg/m³	2100
Roof-slab specific heat	C_{rs}	J/kgK	880
Solar wall absorbtivity	α_{wl}		0.63
Roof-slab absorbtivity	α_{rs}		0.7
Wall emissivity	ε_{wl}		0.9
Roof emissivity	ε_{rs}		0.91
Internal Building Characteristics			
Lighting heat contribution	$\dot{q}_l$	W/m²	5
Occupancy	N_p	-	1
Sensible heat gain from a human performing office work	$\dot{q}_{p,i}$	W/person	66
Infiltration air flowrate	$ACPD$	-	6
Equipment Heat Load	$\dot{Q}_{he,tot}$	W	5

Table A.2: Design parameters for the sustainable cooling alternatives applied to the one-room building

Sustainable Cooling Alternatives	*Symbol*	*Units*	*Value*
Night Flushing (NF)			
NF air change rate	ACH	#	32
Hour of the day NF activated			24h00
Hour of the day NF deactivated			06h00
Roof-pond (RP)			
RP water thickness	z_{rp}	mm	100
RP water mass	m_{rp}	kg	3600
Water absorbtivity	$\alpha_{s,w}$		0.98
Water emissivity	ε_{rp}		0.9
Water transmissivity	τ_w		0.01
Water reflectvity	ρ_w		0.01
Active Mass Cooling			
Water mass flow rate	$\dot{m}_w$	kg/s	1
Heat resistance between water in tubes and slab	$R_{w,rs}$	m²K/W	0.05
Embedded Pipe Diameter	D_p	mm	20
Pipe Spacing	l_p	mm	300

Table A.3 gives the solar radiation, incident and solar heat gain factors that were utilised in the computer simulation of the one-room building.

Table A.3: Solar radiation, incident angles and solar heat gain coefficients for the exposed surfaces of the one-room building simulation

Direct Normal Solar Radiation, $I_{solar,DN}$ (W/m²)

Time of Day	North	East	South	West	Hor.
0.7:00	0	181	19	0	14
08:00	26	686	0	0	209
09:00	147	751	0	0	431
10:00	266	660	0	0	625
11:00	360	481	0	0	776
12:00	420	250	0	0	870
13:00	440	0	0	6.14	902
14:00	418	0	0	262	868
15:00	357	0	0	491	770
16:00	261	0	0	666	617
17:00	141	0	0	752	420
18:00	21	0	0	677	198

Ground Reflected Radiation, $I_{solar,r}$ (W/m²)

Time of Day	North	East	South	West	Hor.
0.7:00	3	3	3	3	0
08:00	28	28	28	28	0
09:00	52	52	52	52	0
10:00	73	73	73	73	0
11:00	88	88	88	88	0
12:00	98	98	98	98	0
13:00	101	101	101	101	0
14:00	97	97	97	97	0
15:00	87	87	87	87	0
16:00	72	72	72	72	0
17:00	51	51	51	51	0
18:00	27	27	27	27	0

Diffuse Solar Radiation, $I_{solar,d}$ (W/m²)

Time of Day	North	East	South	West	Hor.
0.7:00	10	25	12	9	19
08:00	43	95	41	34	76
09:00	59	107	45	42	93
10:00	70	101	45	45	100
11:00	78	87	47	47	104
12:00	83	42	47	47	104
13:00	85	58	48	59	106
14:00	83	48	48	72	106
15:00	78	47	47	88	104
16:00	69	45	45	101	100
17:00	58	42	45	107	92
18:00	42	34	40	94	75

Solar Incident Angle, θ (degrees)

Time of Day	North	East	South	West	Hor.
0.7:00	0	8	84	0	86
08:00	88	17	0	0	73
09:00	80	31	0	0	61
10:00	74	46	0	0	49
11:00	68	61	0	0	38
12:00	65	75	0	0	29
13:00	64	90	0	90	26
14:00	65	0	0	75	30
15:00	69	0	0	60	38
16:00	74	0	0	45	49
17:00	81	0	0	31	61
18:00	88	0	0	16	74

Solar Heat Gain Coefficients

Incident Angle	
Diffuse	0.73
0-40	0.81
40-50	0.8
50-60	0.78
60-70	0.73
70-80	0.62
80-90	0.39

Figure A.1 and Figure A.2 gives the ambient air temperature and relative humidity employed in the computer simulation of the one-room building questionnaire:

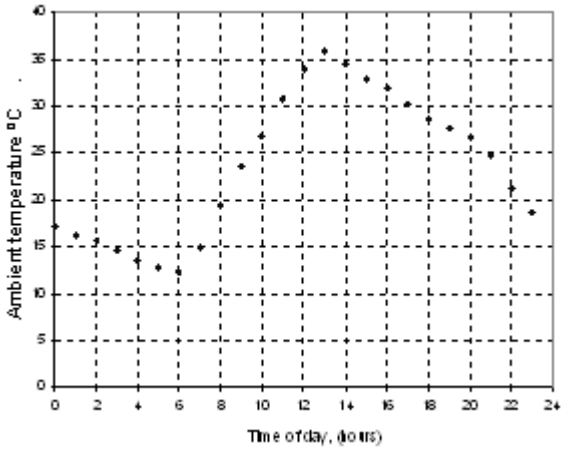

Figure A.1: Ambient temperature employed in the simulation of the one-room building

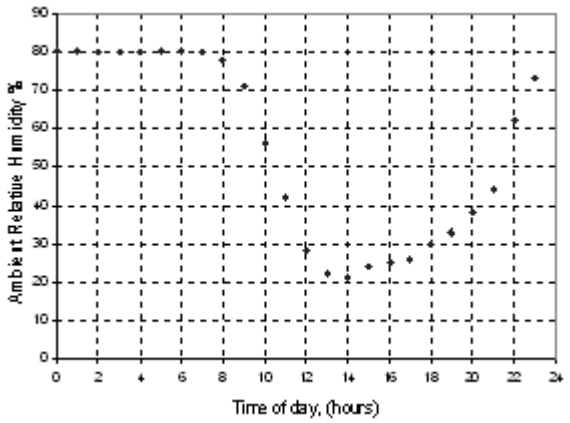

Figure A.2: Relative humidity employed in the simulation of the one-room building

Acknowledgements

This work was supported by KV3 Engineers and the Adaptive Engineering Group, Stellenbosch University.

References

Abernethy, D., (1984). Evaporative roof cooling: A simple solution to cut cooling costs, Proceedings of the Second Symposium on Improving Building Systems in Hot and Humid Climates, College Station, Texas, 24-26 September, pp. 98-102.

Artmann, N., Manz, H. & Heiselberg, P., (2008). Parameter study on performance of building cooling by night-time ventilation, *Renewable Energy*, Vol. 33, pp. 2589-2598.

ASHRAE (2005) ASHRAE Handbook – Fundamentals, American Society of Heating, Refrigerating and Air-conditioning Engineers, Atlanta, Georgia.

Blondeau, P., Sperandio, M. & Allard, F., (1997). Night ventilation for building cooling in summer, Solar Energy, Vol. 61, pp. 327-335.

Carrasco, A., Pittard, R., Kondepundi, S.N., & Somasundaram, S., (1987). Evaluation of a direct evaporative roof-spray cooling system, Proceedings of the Fourth Symposium on Improving Building Systems in Hot and Humid Climates, College Station, Texas, 15-16 September, pp. 94-101.

Cengel, Y.A. and Boles, M.A., (2002). *Thermodynamics: An Engineering Approach*, 4th Edition, New York, McGraw Hill.

Chandra, S. and Kerestecioglu, A.A., (1984). Heat transfer in naturally ventilated rooms: Data from full-scale measurements, *ASHRAE Transactions*, Vol. 90, Issue 1B, pp. 211-225.

Chandra, S., Kaushik, S.C. & Bansal, P.K., (1985). Thermal performance of a non air-conditioned building for passive solar air-conditioning: Evaluation of roof cooling systems, *Energy and Buildings*, Vol. 8, Issue 1, pp. 51-69.

Clark, G., (1989). Passive cooling systems, Passive Cooling, Cook J. (Ed.), MIT Press, Cambridge, MA, pp.347-538.

Clements, J.A. and Sherif, S.A., (1998). Thermal analysis of roof-spray cooling, *International Journal of Energy Research,* Vol. 22, Issue 1, pp. 1337-1350.

Corgnati, S.P. and Kindinis, A., (2007). Thermal mass activation by a hollow core slab coupled with night ventilation to reduce summer cooling loads, *Building and Environment*, Vol. 42, pp. 3285-3297.

Dascalaki, E., Santamouris, M., Balaris, C. & Asimakopoulos, D., (1994). Natural convection heat transfer coefficients from vertical and horizontal surfaces for building applications, *Energy and Buildings*, Vol. 20, Issue 1, pp. 243-249.

Finn, D., Connolly, D. & Kenny, P., (2007). Sensitivity analysis of a maritime located night ventilated library building, *Solar Energy*, Vol. 81, pp. 697-710.

Geros, V., Santamouris, M., Tsangrasoulis, A. & Guarracino, G., (1999). Experimental evaluation of night ventilation phenomena, *Energy and Buildings*, Vol. 29, pp. 141-154.

Givoni, B., (1998). Effectiveness of mass and night ventilation in lowering the indoor daytime temperatures, *Energy and Buildings,* Vol. 28, Issue 1, pp. 25-32.

Holder, L.H., (1957). Automative roof cooling, April Showers, Washington, DC, p. 2.

Incropera, F.P. and DeWitt, D.P., (2002). *Fundamentals of Heat and Mass Transfer*, 5th Edition, New York, Wiley.

Jain, D., (2006). Modeling of solar passive techniques for roof cooling in arid regions, *Building and Enviroment*, Vol. 41, Issue 1, pp. 277-287.

Jain, S.P. and Rao, K.R., (1974). Experimental study on the effect of roof-spray cooling on unconditioned and conditioned buildings, *Building Science*, Vol. 9, Issue 9, pp. 9-16..

Kharrufa, S.N. and Adil, Y., (2006). Roof-pond cooling of buildings in hot acid climates, *Building and Environment*, Vol. 43, pp. 82-89.

Kolokotroni, M., Webb, B.C. & Hayes, S.D. (1998). Summer cooling with night ventilation for office buildings in moderate climates, *Energy and Buildings*, Vol. 27, pp. 231-237.

Koschenz, M. and Dorer, V., (1999). Interaction of an air system with concrete core conditioning, *Energy and Buildings*, Vol. 30, pp. 139-145.

Lehmann, B., Dorer, V. & Koschenz, M., (2007). Application range of thermally activated building systems tabs, Energy and Buildings, Vol. 39, pp. 593-598.

Mills, A.F., (2000). Heat Transfer, 2nd Edition, New Jersey, Prentice Hall.

Mull, T.E., (1997). HVAC Principles and Applications Manual, New York, McGraw Hill.

Pfafferott, J., Herkel, S. & Jäschke, M., (2003). Design of passive cooling by night ventilation: Evaluation of a parametric model and building simulation with measurements, *Energy and Buildings*, Vol. 35, pp. 1129-1143.

Pfafferott, J., Herkel S. & Wambsganß, M., (2004). Design, monitoring and evaluation of a low energy office building with passive cooling by night.

Sodha M.S., Govind, D.P., Bansal, P.K. & Kaushik, S.C., (1980). Reduction of heat flux by a flowing water layer over an insulated roof, *Building and Environment,* Vol. 15, pp. 133-140.

Sodha, M.S., Kumar, A., Singh, U. & Tiwari, G.N., (1980). Periodic theory of an open roof-pond, *Applied Energy*, Vol. 7, Issue 4, pp. 305-319.

Thappen, A.B., (1943). Excessive temperature in flat-top building, *Refrigeration Engineering*, Vol. 1, pp. 163.

World business council for sustainability, [Online]. Available: http://www.wikipedia.com/theinnovation-chain. [2009, October 16].

Received 10 March 201; revised 17 June 2011